

Using Decentralized Control Techniques for Interaction Analysis in Hybrid AC/DC Grids

Atsede G. Endegnanew

Lester Kalemba

Kjetil Uhlen

Energy Systems

SINTEF Energy Research

Trondheim, Norway

atsede.g.endegnanew@sintef.no

Abstract: One of the ancillary services that can be provided by Multi-terminal Direct Current (MTDC) grid to connected ac grids is power oscillation damping (POD). However, using PODs at multiple terminals of an MTDC grid results in multi-loop, multi-variable control system. Such control systems inherently have control loop interactions challenge, which can result in reduced performance of one or more controllers. This entails that PODs installed at multiple converter terminals to damp oscillations in respective ac grids could be affected due to unfavorable interactions among the controllers. Thus, compromising the stability of the connected ac grids. This paper presents analyses of interaction between multiple POD controllers installed on MTDC. For a three-terminal study system, insights on interactions between POD controllers at two different converter terminals of an MTDC are obtained using relative gain array and performance relative gain array measures.

Index Terms: Decentralized control, MTDC, RGA

I. INTRODUCTION

Typically, large synchronous generators provide damping torque to damp low frequency power oscillations in power systems. However, with large penetration of renewables into ac grids and proliferation of power electronics interfaced power sources, the capability of providing damping torque from wind farms, High Voltage Direct Current (HVDC) systems and Flexible AC Transmission (FACTS) devices is being incorporated as a requirement in grid codes. To this end, the ENTSO-E Network Code on High Voltage Direct Current Connections (NC HVDC) [1] specifies that HVDC systems, both HVDC links and Multi-Terminal Direct Current (MTDC) grids, shall be capable of contributing to the damping of power oscillations in connected ac networks.

Research works focusing on providing additional damping torque to ac grids through power oscillation damping (POD) controllers installed on HVDC or MTDC grid converters are found in the literature [2-7]. Provision of power oscillation damping torque from wind farms is discussed in [2-5]. If offshore wind farms are connected to onshore grid via an HVDC link, then a POD controller can be installed either on the offshore wind turbines, or on the onshore HVDC converter station, or a combination of both [3-5]. In the context of POD controllers installed at MTDC terminal converters, their reference settings can be adjusted in such a way that their

effect is maximized. Ref [3] discusses a scenario where a POD controller is installed at one of the terminals of an MTDC grid that interconnects offshore windfarms and asynchronous ac grids. When the wind farm participates in power oscillation damping of one ac grid, where the POD controller is installed, the other asynchronous ac grids experience a disturbance due to dc voltage variation that results from the action of the POD controller. To mitigate dc grid voltage variation, [3] suggests sending the same POD signal but with opposite sign to an offshore wind farm controller. Similarly, [6], which assesses embedded MTDC, proves analytically that similar gain values, but with opposite signs, improve power oscillation damping in the ac grid when POD controllers are installed at more than one terminal in the MTDC grid. Ref [7] presents a decentralized structure for power oscillation damping using MTDC grids. The control structure maximizes the relative controllability by using dc voltage closed-loop shaping. A POD controller is installed at one terminal, and the other terminals react only on the dc voltage change.

Previous works have focused on providing and maximizing power oscillation damping from embedded MTDC grids and from offshore wind farms via HVDC systems. However, using PODs at multiple terminals of an MTDC grid results in multi-loop, multi-variable control system. Such control systems inherently have the challenge of control loop interactions, which can result in reduced performance of one or more controllers. This paper analyzes the effect of POD controller interactions on the overall stability of the hybrid ac/dc power system. The analysis is based on relative gain array (RGA) and performance relative gain array (PRGA), which are techniques used in decentralized controller design to measure the extent and characteristics of interaction among multiple control loops.

The rest of the paper is organized in four parts. In Section II, aspects of power system modelling for small signal stability analysis are described. In Section III, selection of feedback stabilizing signals for the POD controllers, and details of interaction measures used in this work, i.e. RGA and PRGA, are presented. Section IV introduces the case studies and discusses the results of the analyses. Finally, the conclusions are presented in Section V.

II. HYBRID AC/DC POWER SYSTEM MODELLING

In hybrid ac/dc power systems one or more synchronous areas are connected to the same dc transmission system. The

system is complex and non-linear system where differential and algebraic equations (DAE) are used to model different components and their controllers. In small signal stability studies, the non-linear DAE equations are linearized to form a linear state-space representation of the system, given by:

$$\begin{aligned}\Delta \dot{\mathbf{x}} &= \mathbf{A}\Delta \mathbf{x} + \mathbf{B}\Delta \mathbf{u} \\ \Delta \mathbf{y} &= \mathbf{C}\Delta \mathbf{x} + \mathbf{D}\Delta \mathbf{u}\end{aligned}\quad (1)$$

where \mathbf{A} , \mathbf{B} , \mathbf{C} , and \mathbf{D} are state, input, output and feed-forward matrices, respectively, and $\Delta \mathbf{x}$, $\Delta \mathbf{u}$, and $\Delta \mathbf{y}$ are state, input and output vectors, respectively. Eigenvalues and eigenvectors of state-matrix \mathbf{A} are used in small signal stability analysis.

A. AC grid

A sixth-order model [8] is used for detailed representation of synchronous machines with damper windings on both d - and q rotor axes. The ac network representation considers generators as sub-transient emfs behind sub-transient reactances, while converters are represented by controlled voltage sources behind filter impedances. For load flow calculations, the series connected voltage sources and impedances are converted to Norton equivalent current sources in parallel with impedances. The parallel impedances, at generator and converter buses, are augmented to the grid admittance matrix forming \mathbf{Y}_{Aug} to solve the overall network load flow according to (2).

$$\mathbf{I} = \mathbf{Y}_{Aug} \mathbf{V} \quad (2)$$

where \mathbf{I} is generators' and converters' current injection vector, and \mathbf{V} is ac bus voltage vector. In order to capture the relevant dynamics of the ac grids, in the simplest possible way, turbine/governor and excitation system models are used.

B. MTDC converter control

MTDC grids can operate in various types of active power and/or dc voltage control modes such as master-slave, voltage margin, dc voltage droop and dead-band droop control modes. DC voltage droop control is a distributed type of control where more than one terminals participate in active power and dc voltage control. In this control mode, there is linear relationship between the power flow and the dc voltage determined by dc voltage droop constant.

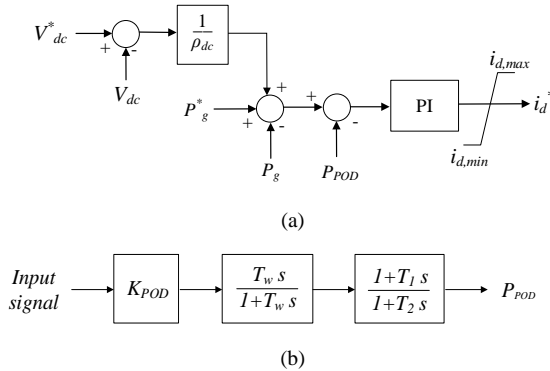


Figure 1. Control structure for (a) DC voltage droop on active power control, and (b) POD on MTDC converters

Figure 1. (a) shows block diagram of an outer loop of an MTDC converter controller with dc voltage droop on active power control. In the figure, the superscript * indicates reference signals, and V_{dc} , P_g , and i_d are dc voltage, active power and d-axis current, respectively. P_{POD} is output of the POD controller that is presented in the next subsection. DC voltage droop control in MTDC neither requires communication nor is dependent on a single terminal. For these reasons, it is considered the most appropriate type of control mode for MTDC grid operation.

C. Power Oscillation Damping controllers on MTDC

The control structure of power oscillation damping (POD) controller on a VSC terminals of an MTDC grids is similar to power system stabilizer (PSS) in excitation system of synchronous generators in ac grids. Figure 1. (b) shows a block diagram for a POD controller for MTDC converters. K_{POD} is gain constant, T_w is wash-out filter time constant, while T_1 and T_2 are lead-lag time constants. Input to the POD controller is a signal where the oscillation to be damped can be observed well. Methods for selection of an input signal for the POD are discussed in detail the next section. The output of the POD (P_{POD}) modulates the active power reference in the outer control of the MTDC converter as shown in Figure 1. (a). In principle, POD on a VSC can modulate either the active power or reactive power reference. However, it was shown in [4, 5, 9] that active power modulation gives better damping and is not sensitive to AVR settings or local voltage variations.

III. SELECTION OF FEEDBACK STABILIZING SIGNALS AND THE CONTROL LOOP INTERACTION MEASURES

A. Geometric measures for controllability and observability

An important step in POD design process is selection of input signal that has high controllability and output signal that has high observability of the mode of interest. Transfer function residue is typically used for the selection of feedback stabilizing signals and the location of PODs. However, given the fact that residues involving signals of different scales and units, such as frequency and voltage angle, cannot be compared with each other due to scaling issues, geometric measures for controllability and observability were proposed in [10]. Geometric measures indicate controllability of a mode from an input and observability of a mode in an output. They are mathematically defined as the cosine of the angle between subspaces spanned by the eigenvectors of state matrix \mathbf{A} , and input/output vectors in state equation (1) Assume that ϕ_i and ψ_i are right and left eigenvectors of matrix \mathbf{A} associated with mode λ_i , respectively. Then, the geometric measures for observability (m_{oi}) and controllability (m_{ci}) of the mode on the l th row of the output vector (\mathbf{c}_l), and from k th column of the input vector (\mathbf{b}_k), respectively, are defined as:

$$m_{ci}(k) = \cos \left[\theta(\psi_i^T, \mathbf{b}_k) \right] = \frac{|\psi_i \cdot \mathbf{b}_k|}{\|\psi_i^T\| \cdot \|\mathbf{b}_k\|} \quad (3)$$

$$m_{oi}(l) = \cos \left[\theta(\mathbf{c}_l^T, \phi_i) \right] = \frac{|\mathbf{c}_l \cdot \phi_i|}{\|\mathbf{c}_l^T\| \cdot \|\phi_i\|}$$

$| |$ indicates absolute value and $\| \|$ indicates 2-norm. If the vectors are orthogonal, i.e. $\theta = 90^\circ$, then there is low observability of the mode on the output and/or controllability from the input. The product of the controllability and observability measures gives a joint geometric observability and controllability measure (m_{coi}) [11].

$$m_{coi} = m_{oi}(l) \cdot m_{ci}(k) \quad (4)$$

A relative large value m_{coi} indicates the most effective input-output signal combination among the alternatives being considered. As m_{coi} is independent of scaling, input-output signals of different units can be compared.

B. Interaction analysis based on de-centralised control theory

The power system is a multiple-input, multiple-output (MIMO) with large number of state variables that can be manipulated to achieve a desired level of system performance. A characteristic feature of MIMO system with multiple control loops is the presence of interactions among various control loops, i.e. each manipulated variable can simultaneously affect several controlled variables. Consider the MIMO transfer function, $G(s)$ given by:

$$G(s) = \begin{bmatrix} g_{11}(s) & g_{12}(s) & \dots & g_{1m}(s) \\ g_{21}(s) & g_{22}(s) & \dots & g_{2m}(s) \\ \vdots & \vdots & \ddots & \vdots \\ g_{m1}(s) & g_{m2}(s) & \dots & g_{mm}(s) \end{bmatrix} \quad (5)$$

where $g_{ij}(s)$ is the transfer function between input u_j and output y_i . For convenience, it is assumed in (5) that $m=n$ such that a single controlled variable is paired with a single manipulated variable via a single feedback controller $G_{ci}(s)$. In general, a change in a manipulated variable, say u_l , will affect several or all of the controlled variables to different degrees due to control loop interactions. When significant process interactions occur, selection of the most effective control configuration may not be so obvious. In such instances, decentralized control techniques can be applied to analyze possible interactions among control loops. In this work, relative gain array (RGA) and performance relative gain array (PRGA) are used to study control loop interactions, and are briefly described below.

C. Relative gain array (RGA)

For a multi-variable plant $G(s)$, and for a particular input-output pair u_j - y_i , the RGA is given by the ratio of the uncontrolled gain (i.e. with all other loops open) and the controlled gain (i.e. with all other loops closed with perfect control). The RGA is obtained using the mathematical relationship in (6).

$$RGA(G(0)) = K(G(0)) = G(0) \otimes (G(0)^{-1})^T \quad (6)$$

where \otimes denotes element-by-element multiplication or Hadamard product. The RGA, \mathbf{K} , is a matrix and each RGA element κ_{ij} is defined as:

$$\kappa_{ij} = \frac{\left(\frac{\partial y_i}{\partial u_j} \right)_{\text{all other loops open}}}{\left(\frac{\partial y_i}{\partial u_j} \right)_{\text{all other loops closed}}} = [G]_{ij} [G^{-1}]_{ji} \quad (7)$$

The RGA, as first proposed in [12], was used as steady-state interaction measure and was frequency independent. However, it was shown in [13] that the RGA depends on frequency, and this was referred to as dynamic RGA (DRGA). At $s=0$, $G(0)$ represents the plant at steady-state, while the DRGA can be visualized in the frequency domain.

D. Performance relative gain array (PRGA)

The concept of PRGA was first proposed in [14], for the design of decentralized controllers based on the independent design approach. Considering a square $m \times m$ multivariable plant, $G(s)$, it is possible to rearrange the elements of $G(s)$ such that the paired elements are along the diagonal of $G(s)$. The decentralized feedback controller transfer function, $G_c(s)$, is then a diagonal matrix. The matrix consisting of diagonal elements of $G(s)$ is given as:

$$\tilde{G}(s) = \text{diag} \{ G_{ii}(s) \}, i = 1, 2, \dots, m \quad (8)$$

With decentralized feedback control, the interactions are then given by off-diagonal elements of the difference $G(s) - \tilde{G}(s)$. The PRGA is calculated as matrix multiplication as [13]:

$$\Gamma = \tilde{G}(s) G^{-1}(s) \quad (9)$$

The PRGA is frequency dependent. At frequencies where feedback is effective, large PRGA elements, compared to 1 in magnitude, entail that the interactions “slow down” the overall response [13]. Small PRGA elements, compared to 1, mean interactions augment performance. $\Gamma = 1$ entails perfect decoupling.

PRGA differs from the RGA/DRGA in that the PRGA gives information on “one-way interaction” between loops, i.e. it provides an indication of the nature as well as the extent of interactions. On the other hand, RGA gives information on “two-way interaction”, i.e. it is merely indicative of the existence of interaction.

IV. CASE STUDY

A. Study system description

A three terminal two level VSC based MTDC grid connecting three asynchronous ac grids as shown in Figure 2. is used as a study system. All three ac grids have multiple generators, and represent large power systems. Matlab/Simulink is used for the analyses. The DC grid is a symmetric monopolar system with ± 200 kV voltage rating. The MTDC terminal converters are operating in dc voltage droop control mode with 4% droop constant.

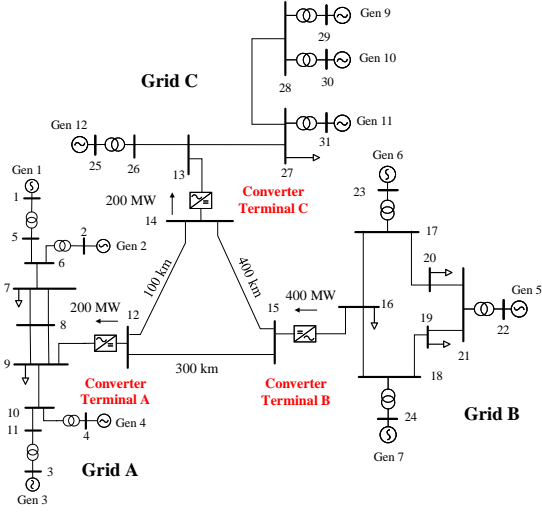


Figure 2. Study system

TABLE I. lists the poorest damped inter-area eigenvalues in Grid A and Grid C. To damp these modes, POD controllers are installed on MTDC grid terminals A and C.

TABLE I. INTER AREA MODES WITH DAMPING RATIO LESS THAN 5%

Mode	Eigenvalue	f [Hz]	ζ [%]	Dominant state variables
λ_A	$-0.04 \pm j3.6$	0.57	1.2	$\delta_{A1}, \delta_{A2}, \Delta\omega_{A3}, \Delta\omega_{A4}, \Delta\omega_{A1}$
λ_C	$-0.14 \pm j3.1$	0.50	4.6	$\delta_{C3}, \Delta\omega_{C4}, \Delta\omega_{C1}, \Delta\omega_{C2}, \Delta\omega_{C3}$

B. POD input-output signal selection

Geometric measures are used to find the most effective control loop for damping of the inter-area modes. Active power reference (P_{ref}) of the converters is the input signal while the locally measured frequency (f_{pll}), PCC voltage (v_{pcc}) and PCC voltage angle (θ_{pll}) are taken as alternatives for output signals. The normalized geometric measure values of the possible input-output signal combinations are presented in TABLE II. The control loop $P_{ref}-\theta_{pll}$ has the highest controllability/observability for the inter-area modes in Grid A and Grid C. Therefore, the PODs at both converter A and C have PCC voltage angle of the respective grids as feedback stabilizing signal.

TABLE II. NORMALIZED GEOMETRIC MEASURES (M_{co}) FOR INTER AREA MODES IN GRID A AND C FOR DIFFERENT CONTROL LOOPS

Grid	Eigenvalues	$P_{ref} - f_{pll}$	$P_{ref} - v_{pcc}$	$P_{ref} - \theta_{pll}$
Grid A	$\lambda_A = -0.04 \pm j3.6$	0.015	0.082	1
Grid C	$\lambda_C = -0.14 \pm j3.1$	0.002	0.564	1

C. POD interaction analysis

With the selected input-output signal combinations, the MIMO transfer function, $G(s)$, becomes the two-by-two transfer function shown in Figure 3. The diagonal elements $g_{11}(s)$ and $g_{22}(s)$ use local measurement signals and are the control loops that are selected using geometric measures in the previous section. The off-diagonal elements $g_{12}(s)$ and $g_{21}(s)$ would entail the use of measurements from remote grids.

$$G(s) = \begin{matrix} P_{ref,A} & P_{ref,C} \\ \theta_{pll,A} \rightarrow & \begin{bmatrix} g_{11}(s) & g_{12}(s) \\ g_{21}(s) & g_{22}(s) \end{bmatrix} \\ \theta_{pll,C} \rightarrow & \end{matrix}$$

Figure 3. Transfer function for the selected input-output signals

Figure 4. (a) shows the magnitude of DRGA elements for the frequency range 1 to 10 rad/s. The vertical traces show the frequency of the poorly damped inter-area modes. The RGA magnitudes for the diagonal elements of the transfer function matrix ($G(s)$), at the frequencies of interest, are around 1.4. This means that there are some interactions between the two POD input-output loops. An RGA number equal to one indicates no interaction with the other loop, while RGA different from one indicates some interactions. Large RGA elements (5-10, or larger) at frequencies important for control indicate that the plant is difficult to control due to strong interactions [13].

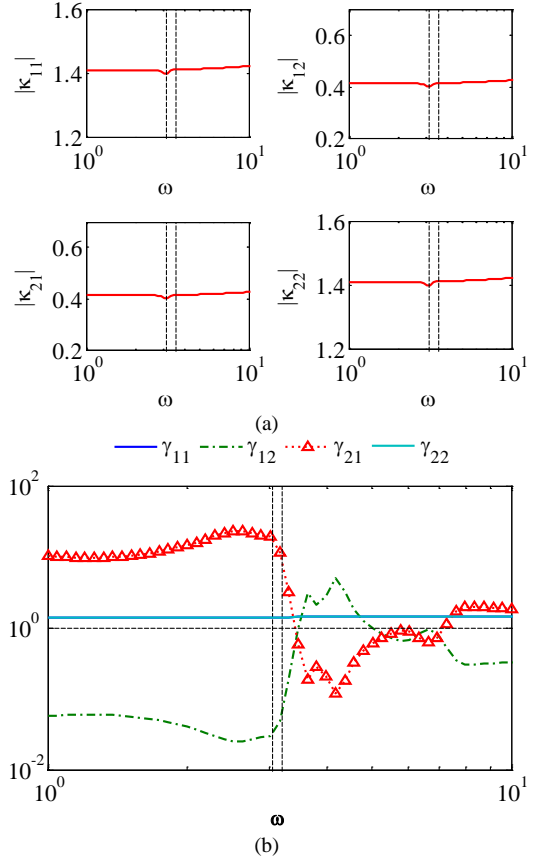


Figure 4. (a) RGA numbers for the selected input-output ($P_{ref}-\theta_{pll}$) pairings, and (b) PRGA

As mentioned in Section III.D, RGA indicates only the existence of interactions while PRGA is also indicative of the extent of interactions. Figure 4. (b) shows that as a result of interaction between the two control loops, the gain of $P_{ref,A} - \theta_{pll,A}$ increases as γ_{12} is less than one while the gain of $P_{ref,C} - \theta_{pll,C}$ decreases as γ_{21} is greater than one, when the two loops

are closed. In other words, loop $P_{ref,C} - \theta_{pll,C}$ enhances the effective gain of loop $P_{ref,A} - \theta_{pll,A}$. On the other hand, loop $P_{ref,A} - \theta_{pll,A}$ reduces the effective gain of the other loop.

D. Modal analysis and POD insertions

Power oscillation damping controllers were added to Terminals A and C to damp the inter-area modes in their respective grids identified in TABLE I. First, the two PODs were tuned individually to damp respective modes of interest, i.e. the POD on Converter A was tuned without connecting the POD on Converter C, and vice versa. Then, both PODs were connected at the same time and interaction between the two control loops was analyzed. TABLE III. shows the damping ratio of the inter-area modes for different cases of POD insertions.

TABLE III. INSERTION OF POD AND DAMPING RATIO OF INTER AREA MODES

Case No.	Description	λ_A	λ_C
		ζ [%]	ζ [%]
Case 1	No POD	1.18	4.35
Case 2	POD on A	11.16	4.32
Case 3	POD on C	1.17	9.61
Case 4	POD on A and C	14.75	6.01

The inter-area modes in Grid A and Grid C had damping ratios of 1.1% and 4.3%, respectively, without POD on the converters. Adding a POD on converter A increases the damping ratio of the inter-area mode in Grid A to 11.1%. Adding a POD only on Converter C improves the damping of the inter-area mode in Grid C from 4.3% to 9.6%. When both PODs on Converter A and on Converter C are used at the same time, the damping ratios of the inter-area modes in Grid A and C become 14.7% and 6%, respectively. This shows that due to the interaction between the two control loops, the effective gain of the POD on Converter A has increased and the effective gain of the POD on Converter C has decreased.

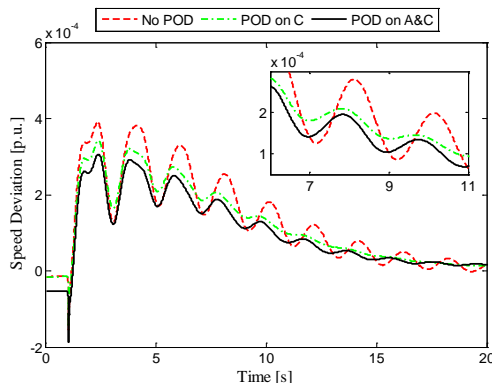


Figure 5. Speed deviation for Gen5 in Grid C

The findings from the eigenvalue analysis are collaborated with time domain analysis. A three-phase symmetric short circuit fault was applied at $t=1s$ at Bus 27 in Grid C. Figure 5. shows rotor speed deviation for Gen5 in Grid C for three different cases analyzed. Without POD installed on Converter C, the speed of the generator has large oscillation following

application of the fault. With POD on converter C only, the oscillation has lower amplitude and is damped out faster. However, when PODs are installed on both Converters A and C, the damping on the interarea mode in Grid C is visibly reduced.

V. CONCLUSION

The paper analyzed interaction between POD controllers on MTDC connecting asynchronous ac grids. Geometric measures of controllability and observability were used to select the most effective input-output signal combinations for the POD controllers. In addition, using RGA and PRGA measures, the interaction between POD controllers at two different converter terminals of an MTDC were assessed. For the analyzed, study case, it was found that due to the interactions the performance of one of the controllers was augmented, while the other deteriorated. The analyses clearly show that care should be take when tuning PODs on converters even though they are connected to different grids.

VI. REFERENCES

- [1] ENTSO-E, "Network Code on High Voltage Direct Current Connections," ed: ENTSO-E, 2016.
- [2] J. L. Domínguez-García, C. E. Ugalde-Loo, F. Bianchi, and O. Gomis-Bellmunt, "Input-output signal selection for damping of power system oscillations using wind power plants," *International Journal of Electrical Power & Energy Systems*, vol. 58, pp. 75-84, 2014.
- [3] M. Ndreko, A. A. van der Meer, B. G. Rawn, M. Gibescu, and M. A. M. M. van der Meijden, "Damping power system oscillations by VSC-based HVDC networks: A North Sea grid case study," in *12th Int. Workshop Large-Scale Integration of Wind Power Into Power Systems as Well as on Transmission Networks for Offshore Wind Power Plants*, 2013.
- [4] Y. Pipelzadeh, N. R. Chaudhuri, B. Chaudhuri, and T. C. Green, "Coordinated Control of Offshore Wind Farm and Onshore HVDC Converter for Effective Power Oscillation Damping," *IEEE Transactions on Power Systems*, vol. PP, pp. 1-1, 2016.
- [5] L. Zeni, R. Eriksson, S. Goumalatos, M. Altin, P. Sørensen, A. Hansen, et al., "Power Oscillation Damping From VSC-HVDC Connected Offshore Wind Power Plants," *IEEE Transactions on Power Delivery*, vol. 31, pp. 829-838, 2016.
- [6] L. Harnefors, N. Johansson, L. Zhang, and B. Berggren, "Interarea Oscillation Damping Using Active-Power Modulation of Multiterminal HVDC Transmissions," *IEEE Transactions on Power Systems*, vol. 29, pp. 2529-2538, 2014.
- [7] R. Eriksson, "A New Control Structure for Multiterminal DC Grids to Damp Interarea Oscillations," *IEEE Transactions on Power Delivery*, vol. 31, pp. 990-998, 2016.
- [8] J. Machowski, J. Bialek, and J. Bumby, *Power System Dynamics: Stability and Control*: WILEY, 2008.
- [9] S. G. Johansson, G. Asplund, E. Jansson, and R. Rudervall, "Power system stability benefits with VSC DC-transmission systems," in *Cigre Session*, 2004, pp. B4-204.
- [10] A. M. A. Hamdan and A. M. Elabdalla, "Geometric measures of modal controllability and observability of power system models," *Electric Power Systems Research*, vol. 15, pp. 147-155, 1988/10/01 1988.
- [11] A. Heniche and I. Kamwa, "Control loops selection to damp inter-area oscillations of electrical networks," in *Power Engineering Society Summer Meeting, 2002 IEEE*, 2002, p. 240 vol.1.
- [12] E. Bristol, "On a new measure of interaction for multivariable process control," *IEEE Transactions on Automatic Control*, vol. 11, pp. 133-134, 1966.
- [13] S. Skogestad and I. Postlethwaite, *Multivariable feedback control: analysis and design* vol. 2: Wiley New York, 2007.
- [14] M. Hovd and S. Skogestad, "Sequential design of decentralized controllers," *Automatica*, vol. 30, pp. 1601-1607, 1994/10/01 1994.